U. S. GEOLOGICAL SURVEY

SAUDI ARABIAN PROJECT REPORT 276

EVALUATION OF MINERALIZATION IN SERPENTINITE AND ENCLOSING ROCKS IN THE HAMDAH AREA, KINGDOM OF SAUDI ARABIA

by

Ronald G. Worl

and

Francoise E. Elsass

U.S. Geological Survey
Open-File Report 81-446

This report is preliminary and has not been reviewed for conformity with U.S. Geological Survey editorial standards. Use of trade names is for descriptive purposes only and does not constitute endorsement by the USGS.

U.S. Geological Survey
Jiddah, Saudi Arabia

1981

The work on which this report is based was performed in accordance with a cooperative agreement between the U. S. Geological Survey and the Ministry of Petroleum and Mineral Resources, Kingdom of Saudi Arabia.

CONTENTS

ILLUSTRATIONS

TABLES

EVALUATION OF MINERALIZATION IN SERPENTINITE AND ENCLOSING ROCKS IN THE HAMDAH AREA, KINGDOM OF SAUDI ARABIA

by

Ronald G. Worl
and
Francoise E. Elsass[1]

ABSTRACT

Serpentinites in the Hamdah area are the southernmost of a series of serpentinite bodies aligned along the Jabal Ishmas-Wadi Tathlith fault zone, a major north-trending structure that extends 250 km to the north and 100 km to the south. In the Hamdah area, serpentinite is in flat sheet-like bodies whereas to the north, it is in highly sheared pods within fault strands. The serpentinite sheets overlie concordantly a metamorphic unit of hornblende schist, quartz-biotite schist, and carbonaceous schist. Structure and lithologies within this unit are continuous and generally not complicated. The serpentinite is overlain disconcordantly by a metamorphic unit that is structurally and lithologically complex. Much of this unit is metaandesite, metagraywacke, and foliated gabbro to diorite but the unit also includes numerous other lithologies.

The original ultramafic rocks were of two types, metamorphic peridotite and a cummulate complex composed of peridotite and minor pyroxenite. Serpentinization was nearly pervasive, but original textures are well preserved and olivine and pyroxene ghosts can be identified. Chrysotile and lizardite are the serpentinite minerals; associated minerals are talc, calcite, chlorite, and amphibole. Minerals of the spinel group - chromite, magnetite, hercynite, and spinel - constitute several percent of the rock. The serpentinite came from alpine-type, harzburgite-subtype, ultramafic bodies that may be the ultramafic portion of an ophiolite. The other lithologies that define an ophiolite are present in the overlying group of metamorphic rocks but only as discontinuous blocks; this relationship suggests that if this suite is an ophiolite, it is fragmented.

A total of 908 samples were taken of serpentinite and enclosing rocks for analytical work. Results indicate that the potential for discovery of economic chromite deposits is small although the geologic environment is correct. There is no potential for nickel-copper sulfide deposits within the serpentinite. Gold was not detected in serpentinite, except in hydrothermal alteration zones at ancient mine sites (Helaby and Worl,

[1] Saudi Arabian Directorate General of Mineral Resources, Jiddah, Saudi Arabia.

1981), but was detected in trace amounts in the enclosing layered rocks. One zone of mixed layered rock and dike rock is worthy of further investigation.

INTRODUCTION

The Hamdah serpentinite area (fig. 1), hereinafter known as the serpentinite area, is between lats 18°50' and 19°10'N. and longs 43°35' and 43°50'E. The village of Hamdah was destroyed by flood waters in approximately 1972, and the name now applies to the general region and specifically to an area of small farms along Wadi Tathlith just north of the map area (plate 1). Wadi Tathlith, the main drainage in this part of the shield, drains northward, but carries water only intermittently. Tathlith, the major commercial center, is approximately 60 km north. The main access to the area is from Khamis Mushayt along a poorly graded road that crosses Wadi Tathlith a few kilometers northwest of the Hamdah area and continues northward. A desert track from Najran in the south to Bishah, Tathlith, and Wadi Dawasir in the north, crosses the area and intersects the Khamis road south of Tathlith. Landforms are mostly isolated granite mountains sticking through pediment surfaces, rounded hills of serpentinite, and rugged angular mountain masses of metamorphic rocks. Altitudes range from approximately 1300 m along Wadi Tathlith to 1600 m or higher in the southeastern part of the area.

Numerous workers have visited the serpentinite area to evaluate asbestos and magnesite deposits. Their studies are summarized in Rooney and Al-Koulak (1979), who did the most recent evaluation of the serpentinites for asbestos. Overstreet (1978) and Warden (1969) mapped respectively the Hamdah (sheet 19/43 D) and Markas (sheet 18/43 B) 30-minute quadrangles. Their reports describe the serpentinite occurrences but only briefly mention the metal content of the serpentinite. Several ancient gold mines occur within the serpentinite area. The ancient mines in the Hajrah-Hamdah group (pl. 2) were mapped and sampled in detail and 14 diamond drill holes tested mineralization (Helaby and Worl, 1981). Ancient mines in the Jabal Mahanid group (pl. 2) were mapped and sampled on a reconnaissance scale (Worl, in press).

This investigation stems from a more encompassing study of gold deposits in a north-trending belt that extends 250 km north and 100 km south of the serpentinite area (Worl, in press). Two major groups of gold deposits are in the serpentinite area, the Hajrah-Hamdah and Jabal Mahanid groups (pl. 2). The Hajr mine, one of the Hajrah-Hamdah group, has the most extensive ancient workings in the southern part of Saudi Arabia. Gold mineralization at the Hajr mine and at the Jabal Mahanid group is spatially related to the serpentinite in that it is along the

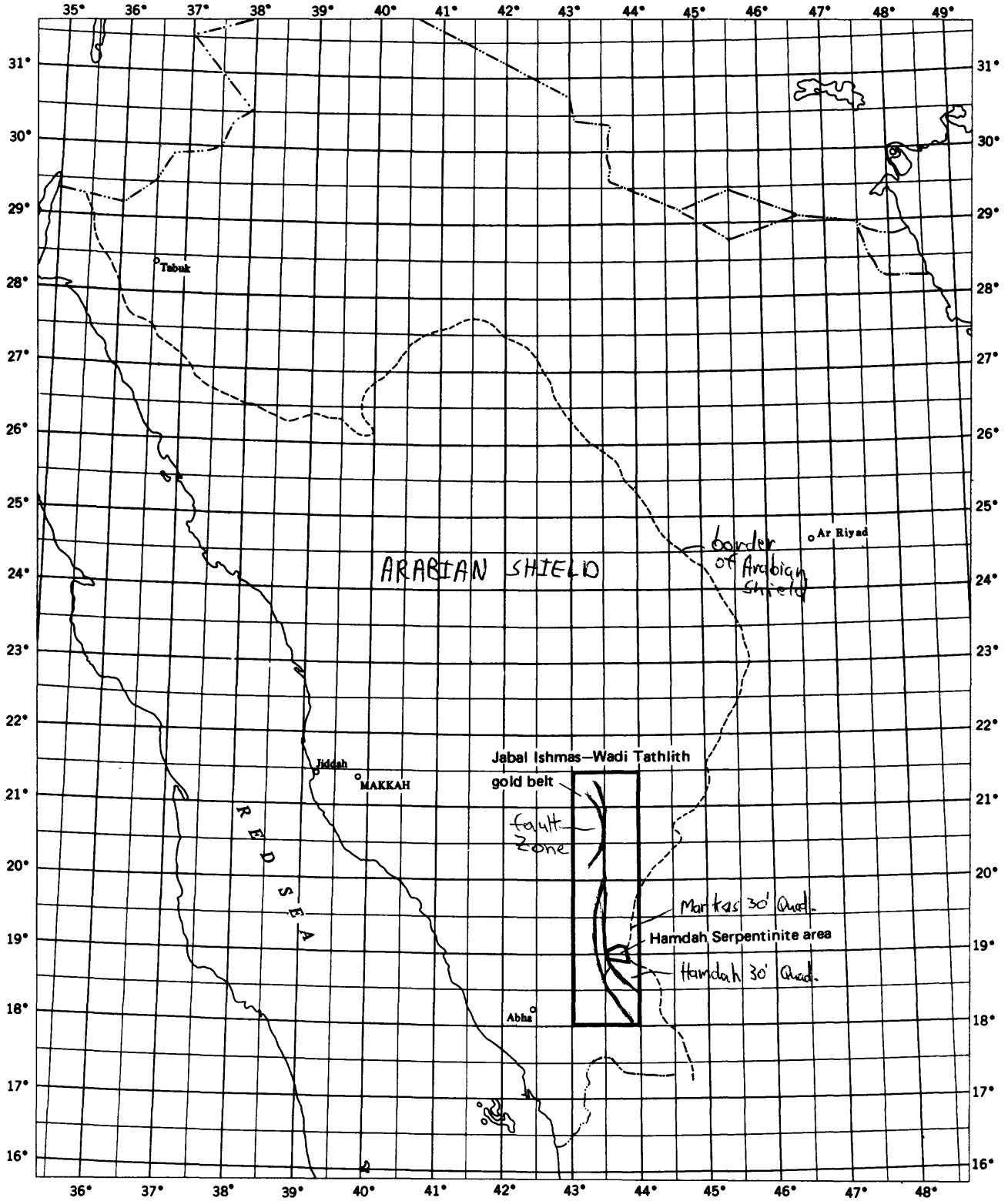

Figure 1. Index map of western Saudi Arabia showing location of the Jabal Ishmas–Wadi Tathlith gold belt and the Hamdah serpentinite area.

contact between the overlying serpentinite and underlying hornblende schist. Gold metallization in these two groups of deposits is hydrothermal in origin and genetically tied to granite, pegmatite, and aplite dikes. The dikes are a late phase of granodiorite, monzogranite, and granite plutons.

The source of the gold carried and deposited by the hydrothermal solutions is unknown. It is conceivable that the gold originally came from a local source and that it was mobilized only for short distances by hydrothermal fluids generated by the intrusives and related dikes. Possible local sources for gold include the serpentinites, carbonaceous schists, porphyritic subvolcanic intrusive and flow rocks, and sulfide-rich zones in greenschist. The fact that only the serpentinites show a spatial relationship to the gold deposits suggests that the source may have been within the serpentinites. In addition to being a possible source for gold the serpentinites generally contain visible chromite, and reconnaissance sampling of several gossans derived from serpentinite detected nickel.

This study was devised to investigate the gold, chromium, and nickel content of serpentinite, the gold content locally of enclosing layered rocks, and the petrologic nature of the serpentinite. Field work was performed during January, July, and August 1977. Mapping was directly on ~ 1:50,000-scale contact prints, enlarged to 1:10,000 where detail was needed. The data were later transferred to a base composed of 1:100,000-scale photomosaics.

Emphasis in mapping was placed upon the serpentinite contact zone and the relationship between serpentinite and the enclosing rocks. Details within the layered rock and intrusive rock sequences and their petrography were studied only in the vicinity of the two groups of ancient mines (Helaby and Worl, 1981; and Worl, 1979). Elsewhere the layered rocks and intrusive rocks were treated in a reconnaissance manner and mapped on the basis of outcrop hand-specimen lithology only. As a consequence considerably more is known of the underlying layered sequence than of the overlying layered sequence and of the felsic intrusive rocks than of the mafic intrusive rocks.

This study was performed in accordance with a work agreement between the U.S. Geological Survey (USGS) and the Ministry of Petroleum and Mineral Resources, Kingdom of Saudi Arabia.

GEOLOGY

Regional setting

The Hamdah serpentinite bodies are the southernmost of a series of serpentinite outcrops along the Jabal Ishmas-Wadi Tathlith fault zone. This major north-trending zone of faulting, shearing, and alteration parallels arcuate north-trending belts of metavolcanic and metasedimentary rocks in crystalline metamorphic and igneous rocks (Worl, 1979). Serpentinite bodies to the north of the Hamdah area are within strands of the fault zone and are highly sheared and deformed pods that locally form the matrix of tectonic melanges. In the Hamdah area, however, serpentinite is in flat sheet-like bodies that extend as much as 40 km east of the major fault zone. The western-southwestern contact of the serpentinite is along a local fault; the major fault is 2 to 10 km to the west.

The Jabal Ishmas-Wadi Tathlith fault zone and serpentinite belt are considered by Frisch and Al-Shanti (1977) as part of the Hulayfah-Hamdah ophiolite belt, which cuts the Arabian Shield in a north-south direction. Schmidt and others (1979) consider this zone to be a suture zone, the Nabitah suture, which was possibly a westward dipping subduction zone for an island arc system of Jiddah age.

Enclosing rocks are part of an andesite-graywacke assemblage that extends southward at least to the Saudi Arabia-Yemen border and northward at least 100 km (Worl, in press). Rocks of this assemblage outcropping in the Malahah quadrangle, 60 km south of Hamdah area, are assigned to the Jiddah group by Greenwood (in press). Regional structural trends in this part of the Arabian Shield are dominantly oriented north and dip or plunge steeply, as does the Jabal Ishmas-Wadi Tathlith fault zone and parallel belts of metamorphic rocks and gneissic rocks. Internal structures within the individual metamorphic belts are at places, but not everywhere, consistent with regional structural trends. Within the Hamdah serpentinite area the major faults and larger igneous bodies trend north. Layering of the serpentinite bodies, however, forms shallow north- or south-plunging folds.

Layered rocks

Layered rocks in the serpentinite zone are mapped as two units on the basis of whether they underlie or overlie the serpentinite. The underlying group is simple in lithology and structure and is in concordant contact with the overlying serpentinite. The overlying group is more complex in that lithologies and structures vary considerably through the area and the rocks are in discordant contact with the serpentinite. The lithologies comprising

each unit have been described in more detail by Worl (in press) and Helaby and Worl (1981).

The underlying group is locally divided into three map units--hornblende schist, quartz-biotite schist, and carbonaceous schist.
Those portions of the underlying group mapped as undivided also have lithologies similar to those described for these three map units. The quartz-biotite-schist unit is composed mostly of medium-grained, highly sheared, quartz-biotite schist with calc-silicate zones and magnetite-rich lenses. Pods and stringers of quartz are common along the foliation. Mineral assemblages include dominant quartz with lesser amounts of biotite, epidote, hornblende, plagioclase, potassium feldspar, muscovite, chlorite, actinolite, magnetite, calcite, and accessory minerals. Interbedded and intergradational with the schist are lenses as much as 100 m thick of hornblende schist, chlorite schist, carbonaceous schist, phyllite, phyllitic quartzite, black marble, quartz porphyry, and dacitic metavolcanic rock.

The hornblende schist unit is composed mainly of fine- to medium-grained, massive to well-foliated greenstones. Foliation is defined by mineral alignment, and is parallel to lithologic layering. Mineral assemblages include hornblende and plagioclase (An_{28-50}) plus epidote, actinolite, and chlorite, any of which may locally be the main mineral constituent, and biotite, quartz, diopside, chlorite, and accessory minerals. Relict clastic texture of lapilli, broken feldspar crystals, and lithic fragments suggests that the original rocks were andesitic pyroclastic rocks and associated graywackes. Bedding is locally graded. The less common, more massive rocks have relict amygdules filled with quartz, epidote, and calcite. Some zones contain bluish quartz phenocrysts that compose more than 10 percent of the rock. Dark-gray marble lenses are minor constituents. Intercalated chlorite and chlorite-sericite schists seem to be mainly along the major north-trending fault zones.

Carbonaceous schist is composed of intercalated lenses of carbonaceous chlorite schist, carbonaceous sericite schist, carbonaceous phyllite, quartz-sericite schist, and thinly bedded dark-gray marble. Exposures are highly foliated with tight folds and contortions, wisps, and thin bands and layers of carbonaceous material. X-ray studies and chemical tests by Mohammad Naqvi and J. J. Matzko, USGS Saudi Arabian Mission, found no evidence of graphite. These rocks are physically and mineralogically similar to carbonaceous schists in the Wadi Bidah district, where studies indicate that the carbonaceous material probably was of algal origin in shallow seas (Kiilsgaard and others, 1978, p. 72). The degree of metamorphism needed to form graphite was apparently not reached in these rocks.

Relict bedding and foliation are generally parallel and define broad open flexural folds around shallow north- or south-plunging axes (pl. 1). The contact between serpentinite and the underlying group parallels layering and conforms to the folding. However, structural complexities in the underlying group increase towards the contact where warped, doubly plunging, mesoscopic folds are common. It is not possible to define structurally homogeneous subareas within this zone. Poles to foliation and to the contact plotted on the lower hemisphere of an equal area net show wide scatter with no distribution pattern (Worl, in press.). Much of the contact zone is sheared, altered, and filled with felsic dikes. Low-angle thrust faults of possible regional significance are exposed in the Hajr mine area. These are semi-concordant to foliation and the serpentinite contact and layering in the underlying group and place rocks of the quartz-biotite schist unit on rocks of the hornblende schist unit. The contact between the underlying group and serpentinite may be a major thrust zone, but relationships are not clear.

The overlying group is lithologically and structurally more complex than the underlying group. The exposures are mainly massive featureless greenstones and fine- to medium-grained greenschists. Pillowed structure and relict amygdules were recognized in a few outcrops, as were lapilli and fragmental crystals. Some of the greenschist in handspecimen seems to be foliated and metamorphosed diorite and gabbro although it may also be metamorphosed graywacke. Mineral assemblages are dominantly chlorite and epidote with lesser amounts of actinolite, green hornblende, plagioclase, potassium feldspar, and quartz. Numerous mafic and ultramafic dikes cut this sequence of rocks and are so abundant locally that they dominate, and the layered rocks occur as screens between the dikes.

Intercalated with the greenstones and greenschists are several lithologies, only two of which are of enough significance to be shown locally as map units: pyritic-carbonaceous schist and brown marble. The pyritic-carbonaceous schist has an extremely fine-grained, black siliceous groundmass that is in part finely disseminated pyrite. Carbonaceous material is as irregular bands and wisps scattered through the rock. Brown marble forms lenses as much as 100 m thick. The thicker lenses are massive, and the thinner lenses are well layered with intercalated lenses of schist. The other lithologies in the overlying group are carbonaceous quartz-sericite schist, phyllitic quartzite, plagioclase amphibolite, and gray-green diopside-tremolite schist. Metamorphism to the greenschist facies is indicated by the presence of actinolite, chlorite, albite, and epidote.

Structure in the overlying group is generally parallel to the numerous mafic dikes that cut this sequence. The contact between serpentinite and the overlying group is sheared, filled with fine-grained mafic dikes, and generally steep. The contact

is discordant to structure in the overlying group, and in many places the serpentinite seems to invade these rocks.

Intrusive rocks

Three groups of intrusive rocks cut all layered rock units and serpentinite: diorite to granite, mafic-ultramafic dikes, and gabbro. Igneous rock names used here follow the classification of the International Union of Geological Sciences (1973).

Diorite is the oldest of the groups and forms small irregular pods, dikes, plutons, and much of the irregular north-trending body in the center of the map area. This rock is generally medium to coarse grained and foliated, and has phenocrysts of amphibole and plagioclase aligned parallel to the foliation. Plagioclase and hornblende are the major minerals, and biotite, pyroxene, and quartz are subordinate. The larger plutons and locally numerous dikes are granodiorite, monzogranite, and granite. The more mafic older phases are medium to coarse grained and porphyritic; the more felsic younger phases are fine grained.

Felsic dikes are common throughout and abundant locally, especially near the Hajrah-Hamdah and Jabal Mahanid ancient mine sites. Most occupy north-, northwest-, or northeast-trending fractures. The dikes are similar in mineralogy to the granodiorite, monzogranite, and granite plutonic rocks with granite being the most abundant. A distinct red garnet can be found throughout the area in plutonic and dike rocks and in related quartz veins. The dikes and related quartz veins are thought to be the source of the gold in the ancient mines at Hajrah-Hamdah and Jabal Mahanid (Helaby and Worl, 1981). The dikes include white, pink, or red granite, graphic granite, felsite, aplite, and pegmatite that grade from one to another along strike.

Mafic-ultramafic dikes are present as individual, narrow to wide dikes continuous for considerable distances or as dike swarms. Fine-grained andesite, locally porphyritic, is most common with lesser amounts of diabase, diorite, dacite, and pyroxenite. Most mafic-ultramafic dikes are cut by felsic dikes and other intrusives although a few andesite dikes are not so cross-cut and are thus apparently the youngest dikes. Many of the mafic dikes are cataclastically deformed, and those within serpentinite show extensive boudinage structure (fig. 2).

Two generations of gabbro are recognized: an older medium- to coarse-grained, foliated variety and a younger fine-grained massive variety in subcircular, at places layered, bodies. The older gabbros are cut by felsic and mafic dikes, but the younger are cut only by andesitic dikes.

Figure 2. Areal view of serpentinite containing numerous rounded boudins of mafic dike rock.

SERPENTINITE

Description

Serpentinite in the Hamdah area occurs as large sheets (fig. 3) overlying one metavolcanic-metasedimentary group and underlying or intruding a second metavolcanic-metasedimentary group, and as smaller lenses, pods, and dikes. The contact between serpentinite and the underlying group is conformable to structure but is generally sheared and altered. Lenses and pods of serpentinite enclosed in rocks of the underlying group are common, but the reverse is not true. In several areas within serpentinite are small exposures of hornblende schist of the underlying sequence; but in all instances the exposure is the core of an antiform and thus a consequence of folding and erosion.

Contact relationships between serpentinite and the overlying sequence are complex. The contact is generally sheared and filled with swarms of mafic dikes, and shows no relationship to structure in the overlying sequence. The serpentinite seems to intrude rocks of the overlying sequence, and pods, lenses, and dikes of serpentinite are locally abundant in the overlying group.

The original ultramafic rocks from which the serpentinites were derived were of two types: metamorphic peridotite and a cumulate complex composed of peridotite and minor pyroxenite. Coleman (1977) describes metamorphic peridotite as rocks within ophiolites consisting primarily of olivine, orthopyroxene, clinopyroxene, and spinel and exhibiting tectonite fabrics. Metamorphic peridotites (harzburgite subtype) occupy the basal parts of ophiolite sequences and are the substrata upon which cumulate ultramafic and gabbroic rocks are deposited. They are included under alpine ultramafic rocks, a broad category as described by Thayer (1960) and Jackson and Thayer (1972). The Hamdah serpentinites fit the category, peridotite bodies of alpine type, harzburgite subtype, of Jackson and Thayer (1972).

Outcrop appearance of the serpentinites varies considerably and is a function of original mineral composition and degree of metamorphism, hydrothermal alteration, and deformation. Primary olivine altered to form reddish-brown serpentine while primary pyroxene produced greenish-gray serpentine. Talc, a common constituent, tends to lighten the color of the rocks and adds a yellowish shade. Hydrothermal alteration produced a mottled reddish-tan rock.

Major shear trends in the serpentinite are shown on plate 1. The metamorphic peridotite is foliated but not layered. Foliation is accentuated by trains of magnetite in millimeter-thick bands along shear planes and microscopically by the ribbon texture of the mesh serpentinite. Regular shaped polyhedrons of serpentinite

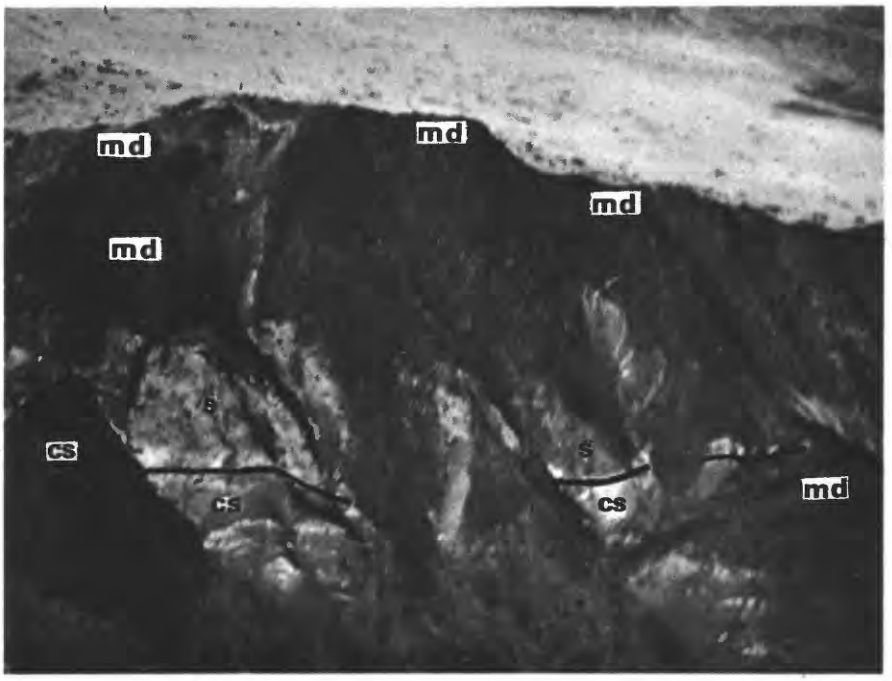

Figure 3. Areal view of serpentinite, carbonaceous schist, and mafic dike.

ranging in diameter from one-half to several centimeters produced by shearing are common. Rocks of the cumulate complex are generally massive.

Mineralogy

Serpentinization of the original ultramafic rocks was nearly pervasive, but relict textures of the original mineral constituents are well preserved. In most samples olivine and pyroxene ghosts can be identified from the serpentine texture (Wicks and Whittaker, 1977). Mesh texture after olivine is common with rims of γ-serpentine and cores of α-serpentine or nearly isotropic material, and sometimes magnetite. Less commonly, fresh relicts of olivine were found as tiny mesh core remnants. Altered pyroxene (enstatite) in longitudinal sections shows finely fibrous serpentine having a uniform orientation along the cleavage traces of the pyroxene crystal. In cross sections the altered pyroxene shows a regular square-shaped mesh texture. The few unaltered pyroxenes found in the metamorphic peridotite are orthopyroxene (enstatite) showing exsolution lamellae of clinopyroxene. Unaltered pyroxenes found in the cumulate complex are clinopyroxenes. Groundmass of the mesh textures is usually fibrous γ-serpentine of pale brown color and irregular extinction.

Chrysotile and lizardite are the only serpentine minerals identified by X-ray analysis; antigorite was not detected. This relationship is not surprising as chrysotile and lizardite are generally more abundant than antigorite in serpentinites except in high-grade metamorphic terranes where antigorite replaces chrysotile and lizardite (Coleman, 1977, p. 98). Minerals associated with chrysotile and lizardite in the serpentinites are talc, locally the major component, amphibole, chlorite, and calcite. Talc in these rocks has three possible origins. Serpentine plus talc can be expected as an alteration product of a rock containing primarily enstatite. Talc-bearing serpentinite can also result from low-temperature alteration of brucite-bearing serpentinite, and finally talc can form as an alteration product of serpentine over a wide range of temperature and pressure (Hemley and others, 1977b). The latter is the preferred explanation of talc in the Hamdah serpentinites. Petrographic observations indicate that talc is a late alteration product and is probably a pseudomorph after serpentine. Brucite was not observed, and in fact talc and brucite are incompatible (Hemley and others, 1977a).

Amphibole is a common constituent, and two varieties are present. The more common is an euhedral, tabular, colorless to pale-green clinoamphibole (cummingtonite), which is a replacement of the primary pyroxene in the cumulate peridotite. It is associated with serpentine or magnesium-chlorite, which replaces

the olivine. A less widespread fibrous white clinoamphibole (actinolite-tremolite) is probably an alteration product developed after serpentine during low-grade metamorphism. The long blades overprint all other silicate minerals present.

Chlorite, which is never abundant, is either grouped around opaque spinel grains or in segregation bands several centimeters thick. Carbonate is a minor constituent as calcite replacing serpentine and as magnesite in veinlets. Alteration of serpentine to carbonate is found mainly in hydrothermal alteration zones associated with felsic intrusives.

Spinel-group minerals found in the serpentinites are chromite, magnetite, hercynite, and spinel. Relict chromite from the ultramafic rocks generally makes up less than 1 percent of the rock as disseminated euhedral grains several millimeters in diameter or as scattered aggregates of small irregular grains. Lenses of chromite a few centimeters thick were recorded at several locations. One float sample from the southeastern-most serpentinite body contains 95 percent coarse chromite. The interstices are filled with magnesium-chlorite. Warden (1969) reports two massive chromite samples from wadi material.

Relict magnetite from the ultramafic rocks has the same crystal habit and distribution as chromite, but generally is in greater abundance, as much as 5 percent of the rock. Secondary magnetite from serpentinization and later alteration can compose as much as 25 percent of the rock as cores of mesh texture after olivine grains, as inclusions in altered pyroxene (bastite), and in segregated bands along shears. The size and shape of the grains are highly variable.

Hercynite spinel is common as small anhedral inclusions in amphibole that has replaced pyroxene in rocks of the cumulate peridotite. The alteration of pyroxene produced amphibole and hercynite (Fe, Al). The abundance of hercynite is low, generally 1 to 2 percent, but locally as much as 5 percent of the rock. The mode of occurrence for hercynite is in mafic and ultramafic rocks where it takes the place of ilmenite in the more normal magnetite-ilmenite assemblage. Spinel *sensu stricto* is observed in most serpentinites, especially those derived from metamorphic peridotite. It is always in minute brownish grains and constitutes less than 1 percent of the rock.

Rodingite has been identified from two sample localities, number 117624 from traverse line G and 127452, a spot sample. One sample was in serpentinite and one was in greenstone close to the contact with serpentinite. Rodingite is a general term applied to metasomatic rocks, such as garnetized gabbro, that are related to tectonic emplacement of the ultramafic rocks and the process of serpentinization (Coleman, 1977, p. 103). All rodingite occurrences in the world have similar diagnostic characteristics. The occurrences associated with the Hamdah

serpentinites are massive dark greenish-gray rocks with elongated orange lenses. The rocks are fine grained and layered and have an allotriomorphic granular texture. The mineral assemblages are of gabbroic type. Diopside is predominant both in segregated bands and as sparsely disseminated small stumpy grains. Plagioclase is andesine to labradorite and occurs as small clear stumpy grains, some of which are twinned. Minor associated minerals are secondary amphibole (fibrous tremolite-actinolite) and chlorite. Sample 127452 contains apatite and sphene as abundant accessory minerals. The other sample contains calcite in the place of sphene. Both contain large lens-shaped porphyroblasts several millimeters long of pink to beige hydrogarnet, the most characteristic mineral of rodingites.

Alteration

The serpentinites are intruded by stocks and dikes of diorite to granite composition (pl. 1). Felsic dikes related to the intrusive stocks are not so abundant in the serpentinite as they are in the underlying metamorphic group. Hydrothermal alteration related to the felsic intrusives is widespread at the contacts with the intrusive bodies and along fractures throughout the serpentinite bodies (fig. 4). Alteration products are of two types: a reddish-tan, carbonate-rich, friable rock and a very dense silicified rock.

Origin

Serpentinites of the Hamdah area were derived from metamorphic peridotites and peridotites having cumulate textures. These are alpine-type, harzburgite-subtype, ultramafic rocks, the lithologies that compose the ultramafic portion of ophiolite sequences (Coleman, 1977, p. 20). The Hamdah serpentinites may represent the ultramafic portion of an ophiolite sequence, but data are not sufficient to be definitive. The other lithologies that together with the ultramafic rocks define an ophiolite sequence are present, but only as isolated fragments in the overlying metamorphic group. It is possible that these fragments of layered gabbro, pillowed volcanic rock, and sheeted mafic dikes are remnants of the constituent parts of an ophiolite sequence that have been tectonically mixed with the overlying metamorphic group.

The nature of the underlying group of rocks and the structure of the footwall zone suggest tectonic transport of the serpentinite sheets. The hornblende schist unit that generally underlies the serpentinite bodies may in fact be a metamorphic aureole of the type commonly found at the base of ophiolite

Figure 4. Hydrothermal alteration of serpentinite along northwest–trending fracture.

slabs (Coleman, 1977, p. 115). This unit is thin, probably less than 200 m, and grades downward away from the serpentinite into quartz-biotite and chlorite schist. Although the contact between serpentinite and the underlying metamorphic group is generally conformable to structure in the underlying group, the structural complexities and inhomogeneities in the underlying group increase towards the contact. Also, within the underlying group are several thrust faults and alteration zones that parallel the contact.

GEOCHEMISTRY

Methods of study

A total of 908 samples were taken of serpentinite and enclosing rocks for analytical work. Sample locations are given on plate 1 and the results are summarized in appendix A. Three types of samples were collected: traverse chip, spot chip, and gravel samples. The traverse chip samples consisted of 2 to 3 kg of chips 2 to 5 cm in diameter taken along a traverse line 20 m in length. A continuing series of samples was taken along the traverse lines set at approximately right angles to the structural trends of the serpentinite and enclosing rocks. The spot chip samples consisted of 2 to 3 kg of chips 2 to 5 cm in diameter taken in an area of serpentinite 20 m in diameter. Gravel samples consisting of 2 to 3 kg of rock fragments 2 to 5 cm in diameter were taken along the traverse lines where there was not sufficient outcrop to collect chip samples.

All analyses were performed by the DGMR (Directorate General of Mineral Resources)-USGS laboratory in Jiddah under the direction of Joe Curry. Each sample was analyzed by semiquantitative spectrographic methods. Selected samples were analyzed by atomic absorption and other chemical methods for copper, lead, zinc, cobalt, nickel, chromium, gold, and silver.

The geochemical data are in a computer-based data file and the DGMR PDP 11/45 computer in Jiddah was used for all editing, retrieval, computations, and statistical studies. This work was performed in cooperation with Gary Selner of the USGS. Judy Stoeser prepared and edited the data file and subset retrieval files. Several standard STATPAC statistical programs were used to summarize the data. Program A470 is designed principally for summarizing and tabulating geochemical data, especially from semiquantitative spectrographic analyses by the USGS and DGMR laboratories. This program assumes that the data are more properly treated on a logarithmic, rather than arithmetic, basis; a valid assumption for most geochemical trace-element data. Cohen's method is used

Table 1.--*Geochemical data subsets*

Group I Serpentinite traverse chip samples*

Sample Traverse	Number of Subset	Sample sequence	Number of Samples
A	1	117400 - 117439	40
B	2	117440 - 117479	40
C	3	117480 - 117499	20
D	4	117500 - 117546	43
F	5	117575 - 117606	25
G	6	117607 - 117654	38
I	7	117665 - 117690	7
L	8	117928 - 117960	17
M	9	117961 - 117999 and 127500 - 127667	151
P	10	127697 - 127881	167
	11	total of 1 through 10	549

Group II Serpentinite gravel samples

	12	117400 - 117999 and 127500 - 127881	126

Group III Serpentinite spot samples

	13	127036 - 127485	73

Includes the following 127 series samples:
036, 157, 332, 364, 366, 367, 369, 371, 372, 373, 376, 377, 382, 385, 388, 391, 395, 396, 397, 398, 399, 400, 401, 402, 403, 404, 406, 408, 409, 410, 411, 412, 413, 415, 416, 419, 420, 421, 423, 424, 425, 427, 429, 430, 431, 432, 433, 434, 435, 436, 438, 439, 440, 442, 444, 445, 447, 448, 449, 450, 454, 455, 456, 458, 459, 460, 461, 462, 463, 464, 468, 484, 485.

Group IV Enclosing rock (mainly layered metamorphic) traverse chip samples

E	14	117547 - 117569	21
J	15	117691 - 117775	85
K	16	117776 - 117801	25
N&O	17	127668 - 127696	29

*The sample sequence begins at the x on the traverse line (pl. 2) and runs consecutively along the traverse line to the finish at the bar. Each sample was taken along a 20 m interval slope distance.

in treating censored distributions to give unbiased estimates of the geometric mean (Miesch, 1967). Program BMD01D computes simple averages and measures of dispersion of selected variables. Program BMD03D computes a simple correlation matrix from selected variables.

The complete data set of 908 samples was divided into 17 subsets (table 1) to facilitate interpretation. Ten subsets are of serpentinite traverse chip samples from separate traverse lines; one subset each for all serpentinite traverse chip samples, all gravel samples, and all serpentinite spot samples; and four subsets for traverse chip samples across layered rocks.

Data synthesis

Analytical results are summarized in appendix A. Each table lists the number of samples, number of analytical values, minimum value, maximum value, geometric mean, geometric deviation, arithmetic mean, and standard deviation for the concentration of each element of interest. The elements of prime concern in this evaluation are chromium, nickel, copper, gold, and silver. As the frequency distributions for these metals generally show moderate to strong positive skewness, the data were transformed to common logarithms and from these, the geometric mean and deviation were determined. The geometric mean is the antilogarithm of the arithmetic mean of the transformed data and is a suitable estimate of relative abundance for comparison purposes, but is not the best estimate of true abundance. Because of a negative bias, it gives values less than true abundance. The arithmetic mean is included as a better estimate of true abundance. Cohen's technique was used to estimate the geometric mean and deviation of censored data (Miesch, 1967). For an example, see titanium and copper of geochemical data subset 1.

Geometric deviation is the antilogarithm of the standard deviation of the data after transformation to logarithms and is a measure of dispersion. The larger the geometric deviation, the wider the base of the distribution curve, thus the larger the dispersion.

Statistical comparisons between the geochemical data subsets were not attempted--comparisons could be made among the 12 geochemical data subsets corresponding to samples in serpentinite and among the 3 geochemical data subsets corresponding to sample traverses across layered rocks.

Chromium values in serpentinite range from 250 to 28,000 ppm. The lognormal curve defined by chromium values is narrow as evidenced by the relative small geometric means, and several values must be considered anomalous for this population (pl. 2).

These anomalous values, however, are widely scattered and do not seem to indicate any general trends. Nickel values in serpentinite range from 20 to 2750 ppm and define a broad lognormal curve as indicated by the high values for the geometric means. Nickel values greater than the mean plus two standard deviations were not detected, and their absence suggests that all values are from one population; thus none is anomalous. Most copper values in serpentinite are low, many less than the detection limit of 5 ppm. Only four samples contain more than 100 ppm copper and only one contains more than 200 ppm. Gold was not detected in serpentinite except at the Hajr mine and Jabal Mahanid group of ancient mines (Worl, 1979). This gold is hydrothermal and related to a series of granite and aplite dikes that intruded the contact between overlying serpentinite and the underlying sequence.

Gold values of the traverse samples taken across the layered rocks are low, ranging from not detected to 1.56 ppm. All samples from geochemical subset 16, traverse K, contain detectable gold and approximately one-half the samples from geochemical subset 15, traverse J, and subset 17, traverses N and O, contain detectable gold, although only in trace amounts. Silver values are also low, ranging from not detected to 2.2 ppm for the traverse samples. Silver was detected in most samples from geochemical subsets 15 and 16 but was not detected in subset 17.

Spearman's rank-correlation coefficients were calculated for each pair of elements using log-transformed data (Mack, 1967) in the serpentinite significant positive correlations are indicated among nickel, cobalt, and magnesium and among calcium, titanium, and barium. Significant negative correlations are indicated between elements of the former group and elements of the latter group. Chromium does not correlate, either positively or negatively, with any other element. The correlation among copper, lead, and zinc is positive. The only significant correlations in the layered rocks are positive among gold, copper, and zinc.

DISCUSSION OF METAL RESOURCE MATERIAL

Geologic environments

Petrology, mineralogy, and trace element content suggest that the Hamdah serpentinites are derived from peridotite bodies of the alpine type, harzburgite subtype (Jackson and Thayer, 1972). The nickel, vanadium, copper, titanium, barium, strontium, cobalt, and chromium content of the Hamdah serpentinites is similar to the trace-metal content of ultramafic peridotite and pyroxenite bodies of alpine type elsewhere in the world (Zonenshain and Kuzmin, 1978; Coleman, 1977; Stanton, 1972).

Alpine-type ultramafic bodies commonly contain massive podiform and sackform chromite deposits. According to Coleman (1977, p. 131) the two modes of occurrence for chromite deposits in ultramafic rocks of this type are: 1) as a random distribution of pods enclosed by dunite within metamorphic peridotite and 2) as pods along the contact between layered gabbro and peridotite. Most of the serpentinite exposures in the Hamdah area are metamorphosed peridotites that contain pods of dunite, many of which in turn contain smaller pods of chromite. Thus, there is a potential for the first type of chromite deposit within the Hamdah serpentinites. However, no layered gabbro in overlying contact with the ultramafic rocks was recognized, so the potential for the second type of chromite deposit appears small.

Nickel in alpine-type ultramafic bodies is usually a minor constituent of olivine and serpentine derived from the former. Nickel concentrations of economic importance are limited to lateritic deposits formed by weathering. Because of the nickel content of some gossans in the area, consideration was initially given to the possibility of nickel-copper sulfide deposits, such as occur in serpentinite in other parts of the world. Subsequent determination of the nature of the original ultramafic bodies essentially eliminated this possibility from consideration.

Known mineralization in the area consists of gold associated with an extensive series of granite dikes (Helaby and Worl, 1981; Worl, 1979). Mineralization is simple and consists of gold disseminated along selvages of granite or aplite dikes, in or along quartz carbonate veinlets, in altered serpentinite - in many places with magnetite, and in silicified quartz-biotite schist. Sulfides are not common; minor arsenopyrite is found at the Hajr mine and locally, sphalerite, chalcopyrite, pyrite, and galena. Gold mineralization is in two geologic settings, both related to granite or aplite dikes. One is directly along the contact between overlying serpentinite and underlying hornblende schist and the other is along bedding or layering in silicified quartz-biotite schist. The hydrothermal solutions carrying the gold were apparently trapped by the relatively impervious serpentinite and spread out along the contact and along layering in the underlying rocks, where the gold was then deposited. The potential of the hydrothermal gold deposits is not under consideration in this paper. A possible local source for the hydrothermal gold from syngenetic gold in the serpentinites and enclosing rocks is under consideration.

Exploration results

The results of the exploration program are not encouraging. Of the three types of deposits under consideration -- chromite in serpentinite, nickel-copper sulfides in serpentinite, or precious

metals in serpentinite or layered rocks -- only the precious metals in layered rocks seem to have any potential.

Chromite pods or lenses more than a few centimeters in width were not noted in the Hamdah serpentinites. The best samples of massive chromite came from wadi gravels. Several anomalous concentrations of chromium, the highest 2.8 percent across 20 m, were detected, but most were individual isolated samples scattered widely through the area, and no obvious trends are indicated. However, two areas defined by the 2500-ppm-chromium contour are worthy of limited further investigation: one in the east-central part of the area and one in the west-central part of the area (pl. 2).

The nickel of the Hamdah serpentinites is probably a nickel silicate. Although not tested, the strong correlation of nickel and magnesium supports this concept in that the magnesium is in silicates. All indications that copper-nickel sulfides might be present are negative. The Hamdah serpentinites are derived from alpine-type perdotite bodies, sulfides were not recorded, and the trace-element chemistry is not typical, especially for chromium (too high) and copper (too low). A system developed by Moeskops (1977) for Australian deposits that uses signatures based upon copper, nickel, zinc, manganese, and chromium to select true gossans from false gossans was applied to the higher nickel values. All of the samples tested fell far outside the true gossan areas on all three diagram plots and the high nickel/copper ratios suggest a non-sulfide source for the nickel. The nickel potential in this zone, therefore, seems to be poor.

Gold was not detected in serpentinite, other than that in hydrothermally altered zones at the ancient mine sites. This gold is hydrothermal in origin and related to granite dikes. Gold was detected in two of the three traverses across layered rocks and in the one traverse across a dike zone. In subset 17, traverses N - O, the sampling was just below the serpentinite contact and the values may be reflecting hydrothermal mineralization along the contact similar to that at the Hajr mine and Jabal Mahanid group of ancient mines (Worl, 1979). The source of the gold in geochemical subset 15, traverse J, is unknown as the zone is sheared and altered and contains serpentinite, mafic dikes, and felsic dikes. Subset 16, traverse K, crosses one of the few exposures of felsic flow rocks in the serpentinite area. There are small ancient workings along silicified breccias and quartz stringers in north-trending shear zones. Numerous dikes that cut the area may be the source of the gold. This zone deserves further investigation.

CONCLUSIONS AND RECOMMENDATIONS

Three types of metallization were under consideration in this investigation: chromite in serpentinite, nickel-copper sulfides in serpentinite, and syngenetic precious metals in

serpentinite or enclosing layered rocks. The geologic environment is correct for podiform chromite deposits--alpine type, harzburgite subtype, ultramafic bodies. However, chromite pods larger than a few centimeters thick were not detected. Results of geochemical sampling of the serpentinites indicate anomalous amounts of chromium in several samples, but these are widely scattered and no trend is indicated. Two areas of serpentinites defined by a 2500-ppm-chromium contour are worthy of limited further investigation for chromium potential, but only in conjunction with other studies.

The nickel in the serpentinites is probably a minor constituent in serpentinite and relict olivine. In alpine-type ultramafic bodies nickel concentrations of economic importance are lateritic deposits, not of consideration in this area. Nickel values obtained from the geochemical samples are not higher than would ordinarily be expected in ultramafic rocks. Copper content is low, often below limits of detection. There seems to be no potential for nickel-copper sulfide bodies in these rocks.

Gold was not detected in serpentinite, other than that in hydrothermally altered zones at the ancient mine sites. This gold is hydrothermal in origin and related to aplite dikes that invade the contact between serpentinite and the underlying metamorphic group. Gold in the enclosing rocks was detected in trace amounts along three traverses. The zone crossed by traverse K (pl. 2), subset 16, is the only one with any potential. A variety of rock types is exposed in this zone, and several small ancient workings are along silicified breccias and quartz stringers in north-trending shear zones. The lithologies and shear zones are continuous for several kilometers north and south. The entire zone is worthy of a more extensive investigation. The other traverses that detected gold in trace amounts, J (pl. 2), subset 15, and N and O (pl. 2), subset 17, cross aplitic granite dikes similar to those at the ancient mine sites. The dikes are probably the source of the trace amounts of gold detected, and neither zone is worthy of further investigation.

Serpentinites of the Hamdah area are not viable targets for chromite, nickel sulfide, or precious-metal deposits. Other possible metal-bearing environments that may be associated with the ultramafic bodies were not investigated. No evidence for disseminated or massive sulfides in pillowed lava sequences or metasedimentary sequences was observed, but neither was it specifically sought. Gold associated with plutonic rocks (Helaby and Worl, 1981) is the best target for exploration, although there is some potential for disseminated gold deposits in layered rocks enclosing the serpentinites.

REFERENCES CITED

Coleman, R. G., 1977, Ophiolites: Springer-Verlag, Berlin-Heidelberg, 229 p.

Frisch, W., and Al-Shanti, A., 1977, Ophiolite belts and the collision of island arcs in the Arabian Shield: Tectonophysics, v. 43, p. 293-306.

Greenwood, W. R., (in press), Geology of the Wadi Malahah quadrangle, sheet 18/43 D, Kingdom of Saudi Arabia: Saudi Arabian Directorate General Mineral Resources Map GM-39, scale 1:100,000.

Helaby, A. M., and Worl, R. G., 1981, Exploration and evaluation of the Hajrah-Hamdah group of ancient gold mines, Kingdom of Saudi Arabia: U.S. Geological Survey open-file report 81-445, 55p., 4pls.

Hemley, J. J., Montoya, J. W., Christ, C. L., and Hostetler, D. B., 1977a, Mineral equilibria in the $MgO-SiO_2-H_2O$ system: I Talc-chrysotile-forsterite-brucite stability relations: American Journal of Science, v. 277, p. 322-351.

Hemley, J. J., Shaw, D. R., and Luce, R. V., 1977b, Mineral equilibria in the $MgO-SiO_2-H_2O$ system: II Talc-antigorite-forsterite-anthophyllite-enstatite stability relations and some geologic implications in the system: American Journal of Science, v. 277, p. 353-383.

International Union of Geological Sciences, 1973, Classification and nomenclature recommended by the IUGS subcommission on the systematics of igneous rocks: Geotimes, v. 18, no. 10, p. 26-30.

Jackson, E. D., and Thayer, T. P., 1972, Some criteria for distinguishing between stratiform, concentric and alpine peridotite-gabbro complexes; 24th International Geological Congress, Sec. 4, p. 289-296.

Kiilsgaard, T. K., Greenwood, W. R., Puffett, W. P., Naqvi, Mohammed, Roberts, R. J., Worl, R. G., Merghelani, Habib, Flanigan, V. J., Gazzaz, A. R., 1978, Mineral exploration in the Wadi Bidah District, 1972-1976, Kingdom of Saudi Arabia: U.S. Geological Survey open-file rept. 78-771, (IR)SA-237, 95 p., 17 figs.

Moeskops, P. G., 1977, Yilgarn nickel gossan geochemistry--a review with new data: Journal of Geochemical Exploration, v. 8, p. 247-258.

Miesh, A. T., 1967, Methods of computation for estimating geochemical abundance: U. S. Geological Survey Professional Paper 574-B, 15p.

Mock, C., 1967, Essentials of statistics for scientists and technologists: New York, Plenum Press.

Overstreet, W. C., 1978, A geological and geochemical reconnaissance of the Tathlith one-degree quadrangle, sheet 19/43, Kingdom of Saudi Arabia: U.S. Geological Survey open-file rept. 78-1072 (IR)SA-230, 139 p., 4 pls., 4 figs.

Rooney, L. F., and Al-Koulak, Z. H., 1979, Asbestos occurrences in serpentinites of the Hamdah area, Kingdom of Saudi Arabia: U.S. Geological Survey open-file rept. 79-360, (IR)SA-239, 24 p., 3 figs.

Schmidt, D. L., Hadley, D. G., and Stoesser, D. B., 1979, Late Proterozoic crustal history of the Arabian Shield, southern Najd Province, Kingdom of Saudi Arabia: King Abdulaziz University Institute of Applied Geology's Symposium on the Evolution and Mineralization of the Arabian-Nubian Shield, Proc., v. 2, p. 41-58.

Stanton, R. L., 1972, Ore Petrology: McGraw-Hill, New York, 713 p.

Thayer, T. P., 1960, Some critical differences between alpine-type and stratiform peridotite-gabbro complexes: International Geological Congress, 21st sess. Copenhagen 13, 247-259.

Warden, A. J., 1969, Interim report on the geology of the Markas area (Asir Province): Saudi Arabian Directorate General Mineral Resources open-file report 350, 142 p.

Wicks, F. J., and Whittaker, E. J. W., 1977, Serpentinite textures and serpentinization: Canadian Mining, v. 15, p. 459-488.

Worl, R. G., 1979, The Jabal Ishmas-Wadi Tathlith gold belt, Kingdom of Saudi Arabia: U.S. Geological Survey open-file rept. 79-1519, (IR)SA-264, 106 p.

Worl, R. G., in press, Gold deposits associated with the Jabal Ishmas-Wadi Tathlith fault zone, Kingdom of Saudi Arabia: Saudi Arabian Directorate General of Mineral Resources Bull.

Zonenshain, L. P., and Kuzmin, M. I., 1978, The Khan-Taishir ophiolitic complex of Western Mongolia, its petrology, origin and comparison with other ophiolitic complexes: Contributions to Mineralogy and Petrology, v. 67, p. 95-109.

APPENDIX

Summary of analytical results

Summaries of analytical data for 16 geochemical data subsets follow. Each summary lists the number of samples in that data set and for each element the number of values (samples containing detectable amounts of that element), minimum value, maximum value, geometric mean, geometric deviation, arithmetic mean, and standard deviation. Values are given in percent for iron, magnesium, calcium, and titanium and in parts per million (ppm) for the other elements. Analyses were by semi-quantitative methods for iron, magnesium, calcium, titanium, manganese, barium, strontium, vanadium, and zirconium and atomic absorption methods for cobalt, copper, nickel, chromium, gold, silver, and zinc.

Table A1.--*Summary of analytical results of all 40 samples from subset 1, traverse A (pl. 2)*

		Number of values	Min	Max	Geometric mean	Geometric dev	Arithmetic mean	Standard dev
Fe	percent	40	0.5	3.0	2.10	1.50	2.23	0.69
Mg	percent	40	2.0	10.0	6.84	1.36	7.10	1.70
Ca	percent	40	0.2	1.5	0.46	1.68	0.63	0.27
Ti	percent	37	0.002	0.02	0.003	2.20	0.008	0.03
Mn	ppm	40	200.	700.	582.9	1.33	602.	134.
Co	ppm	40	91.	128.	122.3	1.10	112.7	10.2
Cu	ppm	16	5.	39.	2.8	3.82	8.4	7.6
Ni	ppm	40	1635.	2750.	2178.	1.13	2193.	262.
Cr	ppm	40	725.	28000.	1504.	1.70	2099.	4213.
Zn	ppm	40	29.	52.	34.7	1.17	35.2	6.0
V	ppm	40	10.	30.	12.2	1.33	12.8	4.4

Table A2.--*Summary of analytical results of all 40 samples from subset 2, traverse B (pl. 2)*

	Number of values	Min	Max	Geometric mean	Geometric dev	Arithmetic mean	Standard dev
Fe (percent)	40	.20	3.0	1.67	1.71	1.84	.68
Mg (percent)	40	1.00	10.0	5.42	1.53	5.8	1.8
Ca (percent)	40	.002	1.5	0.42	2.92	.56	.36
Ti (percent)	27	.002	.015	.003	1.59	.003	.002
Mn (ppm)	39	100.	700.	422.	3.41	530.	186.
Co (ppm)	40	97.	148.	111.4	1.08	111.7	8.9
Cu (ppm)	3	5.0	7.0	--	--	--	--
Ni (ppm)	40	1630.	2410.	2139.	1.09	2145.	170.
Cr (ppm)	40	950	2025.	1479.	1.22	1505.	281.
Zn (ppm)	40	25.	46.	32.8	1.11	33.0	3.5
V (ppm)	28	10.	15.	11.4	1.46	13.1	2.5

Table A3.--*Summary of analytical results of all 20 samples from subset 3, traverse C (pl. 2)*

	Number of values	Min	Max	Geometric mean	Geometric dev	Arithmetic mean	Standard dev
Fe (percent)	20	1.5	3.0	2.51	1.26	2.58	.55
Mg (percent)	20	3.0	7.0	6.48	1.23	6.6	1.1
Ca (percent)	20	0.2	5.0	0.61	2.13	.87	1.06
Ti (percent)	20	0.002	0.2	0.014	5.00	.05	.07
Mn (ppm)	20	500.	1500.	743.	1.32	775.	265.
Co (ppm)	20	33.	117.	94.4	1.35	97.5	20.7
Cu (ppm)	20	5.	119.	18.9	2.52	29.3	32.5
Ni (ppm)	20	270.	2580.	1875.	1.67	2029.	567.
Cr (ppm)	20	750.	2800.	1882.	1.33	1945.	457.
Zn (ppm)	20	22.	43.	28.1	1.19	28.5	5.4
V (ppm)	20	10.	70.	20.9	1.91	26.25	20.8

Table A4.--*Summary of analytical results of all 43 samples from subset 4, traverse D (pl. 2)*

	Number of values	Min	Max	Geometric mean	Geometric dev	Arithmetic mean	Standard dev
Fe (percent)	43	.7	5.0	1.81	1.59	2.0	.95
Mg (percent)	43	3.0	12.5	5.87	1.53	6.4	2.6
Ca (percent)	43	0.1	3.0	0.61	2.11	0.78	0.57
Ti (percent)	40	0.026	0.002	0.02	4.97	0.05	0.06
Mn (ppm)	43	200.	1000.	479.	1.52	520.	208.
Co (ppm)	43	19.	98.	69.4	1.40	72.6	18.3
Cu (ppm)	41	5.	14351.	15.2	3.75	352.0	2185.7
Ni (ppm)	43	420	2575.	1837.	1.49	1947.	530.
Cr (ppm)	43	1000.	3200.	2036.	1.24	2082.	435.
Zn (ppm)	43	19.	1825.	31.0	2.16	76.2	277.5
V (ppm)	43	10.	100.	18.2	1.74	21.9	16.8

Table A5.--*Summary of analytical results of all 25 samples from subset 5, traverse F (pl. 2)*

	Number of values	Min	Max	Geometric mean	Geometric dev	Arithmetic mean	Standard dev
Fe (percent)	25	1.5	5.0	2.88	1.23	2.94	0.6
Mg (percent)	25	7.0	7.0	7.0	1.0	7.0	0
Ca (percent)	25	0.1	3.0	0.32	2.45	0.31	0.64
Ti (percent)	23	0.002	0.015	0.004	2.00	0.006	0.004
Mn (ppm)	25	50.	1500.	610.	1.82	686.	296.
Co (ppm)	25	50.	70.	61.2	1.18	62.0	10.0
Cu (ppm)	25	5.	45.0	9.14	1.78	11.0	8.5
Ni (ppm)	25	105.	205.	152.	1.18	154.	24.
Cr (ppm)	25	1450.	2250.	1800.	1.13	1813.	228.
V (ppm)	25	10.	50.	20.4	1.39	21.6	8.2

Table A6.--*Summary of analytical results of all 38 samples from subset 6, traverse G (pl. 2)*

		Number of values	Min	Max	Geometric mean	Geometric dev	Arithmetic mean	Standard dev
Fe	percent	38	1.0	5.0	2.59	1.40	2.72	0.83
Mg	percent	38	3.0	10.0	7.46	1.28	7.66	1.70
Ca	percent	38	0.3	5.0	0.94	1.95	1.19	0.96
Ti	percent	34	.002	0.10	0.007	4.41	0.02	0.03
Mn	ppm	38	300.	1500.	642.	1.44	687.	279.
Co	ppm	38	20.	70.	58.0	1.31	59.7	12.8
Cu	ppm	20	5.0	10.	4.00	1.37	3.23	2.30
Ni	ppm	38	50.	1750.	140.	1.91	196.	294.
Cr	ppm	38	800.	4300.	1988.	1.41	752.	2105.
V	ppm	38	10.	200	24.8	1.95	31.2	23.2

Table A7.--*Summary of analytical results of all 17 samples from subset 8, traverse L (pl. 2)*

		Number of values	Min	Max	Geometric mean	Geometric dev	Arithmetic mean	Standard dev
Fe	percent	17	1.5	7.0	2.8	1.63	3.12	1.71
Mg	percent	17	7.0	12.5	8.4	1.23	8.41	1.90
Ca	percent	17	0.7	5.0	1.7	1.64	1.91	1.02
Ti	percent	11	0.002	0.1	0.004	3.24	0.009	0.02
Mn	ppm	17	300.	700.	525.	1.36	547.	150.
Co	ppm	17	50.	100.	63.5	1.22	64.7	13.3
Cu	ppm	12	5.0	25.	6.1	1.63	6.5	4.9
Ni	ppm	17	900.	2200.	1775.	1.25	1812.	340.
Cr	ppm	17	900.	2200.	1644.	1.26	2200.	900.
V	ppm	17	10.	200	21.3	1.82	25.9	20.9

Table A8.--*Summary of analytical results of all 151 samples from subset 9, traverse M (pl. 2)*

		Number of values	Min	Max	Geometric mean	Geometric dev	Arithmetic mean	Standard dev
Fe	percent	151	1.5	5.0	2.9	1.26	3.0	0.7
Mg	percent	151	0.7	12.5	7.9	1.35	8.2	2.0
Ca	percent	151	0.007	5.0	0.8	2.54	1.1	0.9
Ti	percent	132	0.003	7.0	0.01	1.10	error	error
Mn	ppm	151	300.	1500.	579.	1.39	607.	176.
Co	ppm	112	15.	110.	92.6	1.25	70.	43.
Cu	ppm	34	5.	20.	5.6	1.49	1.5	3.1
Ni	ppm	151	90.	2550.	1925.	1.48	2014.	417.
Cr	ppm	151	350.	2700.	1274.	1.38	1335.	394.
V	ppm	151	10.	700.	20.1	1.73	26.7	56.8

Table A9.--*Summary of analytical results of all 167 samples from subset 10, traverse P (pl. 2)*

	Number of values	Min	Max	Geometric mean	Geometric dev	Arithmetic mean	Standard dev
Fe (percent)	167	1.0	5.0	2.8	1.38	2.9	0.9
Mg (percent)	167	1.5	12.5	8.4	1.43	8.8	2.8
Ca (percent)	167	0.5	5.0	1.7	1.78	2.0	1.1
Ti (percent)	132	0.002	0.7	0.009	9.87	0.07	0.15
Mn (ppm)	167	300.	1500.	664.	1.34	694.	226.
Co (ppm)	80	10.	115.	71.7	1.60	37.3	42.9
Cu (ppm)	0						
Ni (ppm)	167	20.	2550.	1277.	2.22	1538.	618.
Cr (ppm)	167	300.	4800.	1385.	1.52	1504.	619.
V (ppm)	167	10.	150.	23.6	1.95	30.3	25.3

Table A10.--*Summary of analytical results of 549 samples from subset 11, all serpentinite traverse chip samples*

	Number of values	Min	Max	Geometric mean	Geometric dev	Arithmetic mean	Standard dev
Fe (percent)	549	0.20	7.0	2.57	1.47	2.74	0.95
Mg (percent)	549	0.70	12.5	7.44	1.42	7.84	2.38
Ca (percent)	549	0.002	7.0	0.91	2.56	1.31	1.12
Ti (percent)	464	0.002	0.7	0.01	6.67	error	error
Mn (ppm)	548	50.	1500.	603.	1.45	640.	227.
Co (ppm)	335	10.	148.	87.9	1.42	56.2	48.2
Cu (ppm)	174	5.0	14351.	5.2	3.28	31.0	612.4
Ni (ppm)	549	20.0	2750.	1263.5	2.64	1657.4	748.
Cr (ppm)	549	300.0	28000.	1473.3	1.50	1616.3	1262.0
Zn (ppm)	143	19.	1825.	32.1	1.55	12.0	80.1
V (ppm)	537	10.	700.	20.5	1.85	26.3	36.8

Table A11.--*Summary of analytical results of 126 samples from subset 12, all serpentinite gravel samples*

		Number of values	Min	Max	Geometric mean	Geometric dev	Arithmetic mean	Standard dev
Fe	percent	126	1.5	7.0	3.2	1.40	3.4	1.3
Mg	percent	126	0.7	12.5	6.9	1.37	7.2	1.8
Ca	percent	126	0.5	7.0	1.6	1.73	1.9	1.2
Ti	percent	126	0.005	0.7	0.10	2.27	0.12	0.09
Mn	ppm	126	300.	1500.	714.	1.34	747.	248.
Co	ppm	57	17.	120.	72.7	1.33	33.9	39.0
Cu	ppm	58	5.	500.	10.8	2.48	10.6	45.7
Ni	ppm	126	50.	2400.	889.	2.74	1212.	652.
Cr	ppm	126	200.	4350.	1154.	1.73	1324.	691.
V	ppm	126	15.	150.	49.6	1.68	56.0	25.9

Table A12.--*Summary of analytical results of 73 samples from subset 13 (pl. 2), serpentinite spot samples*

		Number of values	Min	Max	Geometric mean	Geometric dev	Arithmetic mean	Standard dev
Fe	percent	73	1.0	5.0	2.98	1.45	3.18	1.13
Mg	percent	73	1.5	12.5	7.28	1.72	8.14	3.10
Ca	percent	73	0.1	20.0	0.99	4.35	3.08	5.02
Ti	percent	63	0.002	1.25	0.006	4.27	0.04	0.17
Mn	ppm	73	150.	3000.	691.	1.57	773.	461.
Co	ppm	73	30.	140.	91.6	1.35	95.1	22.6
Cu	ppm	0						
Ni	ppm	73	55.	2700.	1513.	2.12	1778.	661.
Cr	ppm	73	250.	7150.	2034.	1.62	2261.	1091.
V	ppm	73	10.	200.	26.7	1.89	34.1	31.2

Table A13 --*Summary of analytical results of all 21 samples from subset 14, traverse E (pl. 2)*

		Number of values	Min	Max	Geometric mean	Geometric dev	Arithmetic mean	Standard dev
Fe	percent	21	3.0	7.0	5.24	1.38	5.48	1.53
Mg	percent	21	1.5	10.0	4.84	1.59	5.31	2.24
Ca	percent	21	0.5	7.0	3.61	1.88	4.19	2.00
Ti	percent	21	0.05	1.25	0.99	1.33	1.02	0.24
Mn	ppm	21	700.	3000.	1661.	1.30	1652.	427.
Co	ppm	21	11.	40.	20.8	1.38	21.9	7.3
Cu	ppm	21	29.	98.	52.	1.40	55.	19.
Ni	ppm	21	83.	2575.	318.	2.72	535.	642.
Cr	ppm	21	500.	1500.	724.	1.42	771.	310.
Au	ppm	ND						
Ag	ppm	ND						
Ba	ppm	21	100.	2000.	426.	1.86	512.	381.
Sr	ppm	21	100.	500.	287.	1.49	307.	112.
Zr	ppm	21	70.	200.	108.	1.32	112.	33.
Zn	ppm	21	20.	80.	35.	1.55	39.	19.
V	ppm	21	50.	500.	118.	1.55	132.	89.

Table A14 --*Summary of analytical results of all 85 samples from subset 15, traverse J (pl. 2)*

		Number of values	Min	Max	Geometric mean	Geometric dev	Arithmetic mean	Standard dev
Fe	percent	85	0.5	10.0	4.17	1.88	4.86	2.20
Mg	percent	85	0.005	7.0	1.13	3.02	1.68	1.15
Ca	percent	85	0.2	7.5	3.71	1.96	4.43	2.50
Ti	percent	85	0.003	1.0	0.33	2.30	0.43	0.26
Mn	ppm	85	70.	5000.	1160.	2.57	1581.	1024.
Cu	ppm	85	6.	555.	66.5	1.86	81.4	68.7
Ni	ppm	85	25.	425.	89.	1.75	106.	77.5
Cr	ppm	85	350.	700.	465.	1.18	471.	81.4
Au	ppm	38	0.05	0.4	0.003	21.36	.06	.05
Ag	ppm	77	0.5	2.2	0.59	3.66	.89	.35
Ba	ppm	85	20.	700.	168.	1.71	190.	92.
Sr	ppm	81	100.	300.	197.	1.49	209.	78.
Zr	ppm	85	10.	150.	63.3	1.62	69.	26.
Zn	ppm	85	10.	270.	38.5	1.83	48.	42.

Table A15--*Summary of analytical results of all 25 samples from subset 16, traverse K (pl. 2)*

		Number of values	Min	Max	Geometric mean	Geometric dev	Arithmetic mean	Standard dev
Fe	percent	25	3.0	7.0	5.3	1.42	5.6	1.7
Mg	percent	25	0.7	7.0	2.6	1.78	3.0	1.5
Ca	percent	25	3.0	7.0	4.6	1.34	4.8	1.3
Ti	percent	25	0.1	0.7	0.4	1.51	0.4	0.3
Mn	ppm	25	700.	1500.	996.	1.29	1028.	272.
Co	ppm	ND						
Cu	ppm	ND						
Ni	ppm	ND						
Gr	ppm	ND						
Au	ppm	25	0.005	1.56	0.10	2.12	0.17	0.30
Ag	ppm	25	0.5	1.6	0.99	1.35	1.02	0.27
Ba	ppm	25	30.	300.	196.	1.72	218.	83.
Sr	ppm	25	100.	300.	191.	1.27	196.	43.
Zr	ppm	24	20.	100.	63.	1.86	71.	29.
Zn	ppm	ND						

Table A16--*Summary of analytical results of all 29 samples from subset 17, traverses N and O (pl. 2)*

		Number of values	Min	Max	Geometric mean	Geometric dev	Arithmetic mean	Standard dev
Fe	percent	29	1.0	5.0	2.36	1.78	2.72	1.35
Mg	percent	29	0.3	1.0	3.07	2.20	3.98	2.85
Ca	percent	29	1.0	7.0	2.81	1.64	3.16	1.62
Ti	percent	29	0.07	0.7	0.37	1.50	error	error
Mn	ppm	29	100.	1500.	959.	1.94	1106.	445.
Cu	ppm	29	15.	70.	41.	1.39	43.	13.
Au	ppm	8	.05	.07	0.0005	39.18	.05	.005
Ba	ppm	24	20.	500.	217.	1.96	210.	128.
Sr	ppm	29	100.	300.	199.	1.60	219.	87.
Zr	ppm	29	10.	150.	61.	2.03	73.	36.
Zn	ppm	29	20.	50.	36.	1.30	37.	9.